Density Functional Theory and QT Atoms-in-Molecules Study on the Hydration of Cu(I) and Ag(I) Ions and Sulfides

Boris Ni and James R. Kramer

School of Geography and Geology, McMaster University, Hamilton, Ontario, Canada

Nick H. Werstiuk*

Department of Chemistry, McMaster University, Hamilton, Ontario, Canada

Received: July 23, 2004; In Final Form: November 25, 2004

The hydrates of Cu^+, Ag^+, CuS^-, AgS^-, Cu_2S, andAg_2S were investigated with density functional theory (DFT), solvent field, and atoms-in-molecules (QTAIM) calculations. We found that covalent bonding of the first-shell water molecules to the metals plays a significant role in the total solvation energy. Molecular graphs were obtained and the bonding characterized by analysis of the electron density and its laplacian at bond critical points. Long-range electrostatic interactions between solute and the bulk solvent, quantified by solvent-field calculations, are more important for hydrated anions CuS^- and AgS^- than for Cu^+ and Ag^+ as well as for the neutral species Cu_2S and Ag_2S. Computed enthalpies of formation for hydrated Cu^+ and Ag^+ correlated well with experimentally determined values and allowed us to characterize the structures of several hydrates studied in the gas phase. We found that the stability of the hydrates is leveled in the water solvent field. The reactions of dissociation and substitution of metal sulfides in the gas phase and in solution were compared. A decrease in the of energy of the reactions in going from the gas phase to solution is explained on the basis of the higher coordination of metal atoms in the first hydration shell.

Introduction

Copper and silver ions and their sulfide complexes play an important role in biochemical reactions of living species. For example, Cu(I) sulfide clusters serve as catalytic centers in biologically important reactions of charge transfer, ligand exchange and oxidative degradation.[1−3] Free or weakly bound Cu(I) and Ag(I) ions are highly toxic to aquatic animals even at low concentrations.[4−7] At the same time, complexation of a metal by sulfide substantially suppresses its toxicity.[8,9] Investigation of the role of metal sulfides in biochemical reactions is often complicated by the lack of knowledge about the molecular structure (bonding) and coordination of hydrates in solution. Differing results regarding the nature of the first hydration shell of Cu^+ and Ag^+ have been published. Feller[10] and Bauschlicher[11] found computationally that two water molecules bind in the first shell of Cu^+ and three to Ag^+. Combined theoretical and experimental work carried out by Dalleska[12] detected up to four water molecules close to Cu^+. Martinez[13] also found four water molecules in the nearest shell of solvated Ag^+, but Curtiss[14] and Armunanto[15] found up to six water molecules coordinated to Cu^+ and Ag^+ in computational studies. The importance of solvation cannot be ignored. Although the experimental gas-phase atomization energies of Cu_2S and Ag_2S[16] (135.9 ± 5 and 107.6 ± 5 kcal mol^{-1}, respectively) demonstrate that Cu(I)−S bonds are stronger than Ag(I)−S bonds, solid Ag_2S is favored over Cu_2S ($\Delta G^0 = 1.8$ kcal mol^{-1}) only marginally in the aqueous standard state.[17] The apparent facile substitution of Cu(II) by Ag(I) in solution reported by Kraus[18] also raises the question about feasibility and possible mechanisms of displacement of Cu(I) by Ag(I). For this reason and our burgeoning interest in characterizing the bonding of Cu(I) and Ag(I) sulfides,[19,20] we undertook a study of the hydration of selected species in the gas phase and in the water solvent field. We carried out a density functional study (DFT) and atoms-in-molecules (QTAIM) study of the molecular structures (bonding) and the thermochemistry of the formation of Cu_2S and Ag_2S hydrates and their products—Cu^+, Ag^+, CuS^-, and AgS^-—obtained upon dissociation. The substitution of Cu(I) by Ag(I) in hydrated sulfides was also explored computationally. The results are presented and discussed in this paper.

Computational Methods

The hydration of Cu(I)− and Ag(I)−sulfides and their dissociation products Cu^+, Ag^+, CuS^-, and AgS^- was modeled by investigating complexes involving a number of water molecules and embedding the complexes in a dielectric continuum—the water solvent field. The molecular complexes, consisting of solute along with coordinated and hydrogen bonded water molecules (the first and partly second shells), were considered explicitly at the ab initio level. Equilibrium optimized geometries and wave functions were obtained at the DFT level implemented in Gaussian 98.[21] Calculations were carried out with Becke−Perdew−Wang (Becke3PW91) exchange-correlation potential.[22] The 6-311+G(d) basis set was used for all elements except Ag because Gaussian 98 does not provide medium size all-electron basis sets for atoms beyond Kr. Given that QTAIM analyses with PROAIM require all-electron wave functions, we used the DZVP orbital basis set for Ag originally developed for the DeMon program.[23] It includes 6s, 5p, 3d functions with contraction (633321/53211*/531+) along with polarization and diffuse functions. Calculations of equilibrium

* Corresponding author. E-mail werstiuk@mcmaster.ca.

10.1021/jp046712j CCC: $30.25
Published on Web 02/08/2005

TABLE 1: Computational and Experimental Equilibrium Bond Distances *R* (Å) and Bond Dissociation Energies *E* (kcal mol^{-1})

	LanlDZ	DeMon	exp[a]
R(Ag−S)	2.404	2.389	2.45
E(Ag−S)	43.5	47.9	50.9 ± 3.5
R(Ag−SAg)	2.409	2.384	2.45
R(Ag−O)	1.992	2.027	2.003

[a] Reference 16.

bond distances and dissociation energies of Ag−S and Ag−O bonds were carried out in order to validate the use of the DeMon basis set for calculations involving Ag−S. The results of all-electron calculations together with those performed with the LanlDZ basis set included in Gaussian 98 are presented in Table 1. The calculated bond distances are similar for both levels of theory and differ from the experimental set only marginally, by no more than 0.06 Å. Interestingly, the dissociation bond energy predicted with DeMon basis for the Ag−S bond is closer to the experimental value than the one calculated at the LanlDZ level. Clearly, the DeMon basis set for the Ag is reliable and compatible with the 6-311+G(d) basis used for the other atoms.

Optimization of weakly bound complexes such as $[MS(H_2O)_n]^-$ and $[M_2S(H_2O)_n]$ with numerous hydrogen bonds required up to 300 SCF calculations because the calculation of forces for noncovalent interactions was close to the limit of precision for ab initio methods. Nevertheless, all optimizations converged, and QTAIM analyses were carried out with AIM2000.[24] Vibration analyses were performed for all complexes in order to obtain enthalpies and free energies for the hydrates and their dissociation. Bulk solution effects were probed by carrying out standard calculations with the dielectric continuum model (SCRF=IPCM) where the default isosurface of the electron density defined the hydrate cavity. The counterpoise correction (CPC) method was used to evaluate the basis set superposition error (BSSE).[25]

Results

Structure of Cu^+ and Ag^+ Hydrates. Studies on the hydration of ions and molecules require information about the coordination and bonding of the chemically important first hydration shell. Questions such as how many water molecules should be included in the first shell and what is the nature of the bonding of the solvated species must be addressed. We began our investigation by studying the $[M(H_2O)_n]^+$ hydrates.[10−15] Specifically, different structures that included a metal cation surrounded by four and six water molecules were optimized to determine the preferred structures, their relative energies, and to gain information on the nature of the bonding. The geometry optimizations successfully converged with the default convergence criteria without the use of symmetry restrictions. Consequently, the structures do not exhibit geometrical parameters that would be expected to be identical if symmetry constraints were imposed. Selected structural parameters of the Cu^+ and Ag^+ hydrates are collected in Table 2 and Table 3, respectively. Three stable structures with four water molecules were obtained for Cu^+ and Ag^+. The Cu^+ species are displayed in Figure 1 as (a), (c), and (e). The coordination—unambiguously defined by the number of bond paths terminating at a nucleus—and the nature of the bonding and between solute and solvent molecules was determined by AIM topological analyses.[26] This obviates the potential inaccuracies that may arise in assigning bonds simply on the basis of interatomic distances.[19] The molecular graphs obtained with AIM2000 are displayed as Figure 1b,d,f. The small spheres in Figure 1 and throughout the Figures correspond to the bond critical points, the properties of which provide quantitative information about covalent bonding. In the case of $[Cu(H_2O)_2(H_2O)_2]^+$ (Figure 1a,b), two water molecules are covalently bonded—two bond paths terminate at Cu^+—in the first shell and two interact with the first-shell water molecules through hydrogen bonds. For three-coordinate $[Cu(H_2O)_3(H_2O)]^+$ (Figure 1c,d), one H_2O is hydrogen bonded to two first-shell H_2Os. The near-tetrahedral hydrate $[Cu(H_2O)_4]^+$ is displayed as Figure 1e,f. The structures of $[Cu(H_2O)_2(H_2O)_2]^+$ and $[Cu(H_2O)_3(H_2O)]^+$ displayed in Figure 1a,c are similar to those reported in ref 10. Hydrate $[Cu(H_2O)_4]^+$, shown as Figure 1e, is analogous to the one reported in refs 12−15. The molecular graphs of the Ag^+ analogues are included in Supplementary Figure 1 as (a), (b), and (c), respectively. The geometrical structures of $[Cu(H_2O)_4]^+$ and $[Ag(H_2O)_4]^+$ are not precisely tetrahedral (the M−O distances are not equal and the bond angles were not exactly 109.47°). In fact, we found that the optimized structures of $[Cu(H_2O)_4]^+$ and $[Ag(H_2O)_4]^+$ with forced D_{2d} symmetry (equal M−O bonds and bond angles of

TABLE 2: Interatomic Distances (Å) and Values of Electron Density (e Å^{-3}) at Bond Critical Points for Cu(I) Hydrates

hydrate	M1−S	M2−S	M1−O1[a]	M1−O2[a]	M2−O3[a]	M2−O4[a]	M2−O10	S−H5	S−H6	O2−H4	O4−H1	O5−H9	O6−H4	O7−H2	O9−H1
$[Cu(H_2O)_2(H_2O)_2]^+$			1.876	1.876							1.617				
			0.658[b]	*0.658*							*0.355*				
$[Cu(H_2O)_3(H_2O)]^+$			2.036	1.967	2.040						1.871				
			0.448	*0.516*	*0.444*						*0.204*				
$[Cu(H_2O)_4]^+$			1.996	2.144	2.177	2.159									
			0.481	*0.356*	*0.334*	*0.346*									
$[Cu(H_2O)_2(H_2O)_4]^+$			1.862	1.862							1.691				
			0.686	*0.686*							*0.296*				
$[Cu(H_2O)_4(H_2O)_2]^+$			2.112	2.112	2.114	2.113							1.902		
			0.382	*0.382*	*0.380*	*0.381*							*0.190*		
$[Cu(H_2O)_6]^+$			2.037	2.037	2.445	2.555									
			0.436	*0.436*	*0.192*	*0.153*									
$[CuS(H_2O)_4]^-$	2.105		2.014					2.167	2.185	1.805	1.616				
	0.699		*0.480*					*0.228*	*0.219*	*0.251*	*0.398*				
$[CuS(H_2O)_6]^-$	2.112		1.994					2.209	2.222	1.807	1.605				
	0.692		*0.503*					*0.203*	*0.193*	*0.245*	*0.407*				
$[Cu_2S(H_2O)_8]$	2.178	2.148	2.304	2.026	1.964	2.667		2.177	2.148				1.924	1.675	
	0.608	*0.651*	*0.270*	*0.469*	*0.545*	*0.141*		*0.212*	*0.225*				*0.188*	*0.330*	
$[Cu_2S(H_2O)_{12}]$	2.215	2.144	2.002	2.226	1.936	3.466	3.118	2.356	2.299			1.849	1.766	1.839	1.717
	0.562	*0.650*	*0.509*	*0.311*	*0.588*	*0.035*		*0.137*	*0.165*			*0.220*	*0.264*	*0.220*	*0.310*
$[AgCuS(H_2O)_8]$	2.159	2.474	2.344	2.009	2.351	2.548		2.069	2.088				1.809	1.675	
	0.634	*0.435*	*0.250*	*0.485*	*0.319*	*0.215*		*0.264*	*0.252*				*0.241*	*0.332*	

[a] For hydrates with a single type of metal atom, M2 = M1. [b] Electron density (e Å^{-3}) at bond critical points given in italics.

TABLE 3: Interatomic Distances (Å) and Values of Electron Density (e Å^{-3}) at Bond Critical Points for Ag(I) Hydrates

hydrate	M1−S	M2−S	M1−O1[a]	M1−O2[a]	M2−O3[a]	M2−O4[a]	M2−O10	S−H5	S−H6	O2−H4	O4−H1	O5−H9	O6−H4	O7−H2	O9−H1
$[Ag(H_2O)_2(H_2O)_2]^+$			2.206	2.206							1.665				
			0.422[b]	*0.422*							*0.318*				
$[Ag(H_2O)_3(H_2O)]^+$			2.334	2.302	2.332						1.891				
			0.319	*0.337*	*0.320*						*0.195*				
$[Ag(H_2O)_4]^+$			2.410	2.409	2.406	2.390									
			0.270	*0.270*	*0.272*	*0.281*									
$[Ag(H_2O)_2(H_2O)_4]^+$			2.177	2.177							1.731				
			0.453	*0.453*							*0.270*				
$[Ag(H_2O)_4(H_2O)_2]^+$			2.394	2.392	2.398	2.394							1.904		
			0.280	*0.281*	*0.278*	*0.280*							*0.187*		
$[Ag(H_2O)_6]^+$			2.464	2.464	2.579	2.591									
			0.238	*0.238*	*0.190*	*0.182*									
$[AgS(H_2O)_4]^-$	2.374		2.380					2.131	2.140	1.801	1.781				
	0.516		*0.304*					*0.246*	*0.241*	*0.252*	*0.377*				
$[AgS(H_2O)_6]^-$	2.384		2.347					2.168	2.182	1.806	1.627				
	0.510		*0.323*					*0.220*	*0.215*	*0.245*	*0.385*				
$[Ag_2S(H_2O)_8]$	2.457	2.458	2.523	2.341	2.347	2.548		2.055	2.059				1.802	1.696	
	0.450	*0.449*	*0.226*	*0.325*	*0.321*	*0.215*		*0.273*	*0.270*				*0.245*	*0.316*	
$[Ag_2S(H_2O)_{12}]$	2.529	2.417	2.283	2.495	2.257	2.987	3.293	2.399	2.322			1.764	1.988	1.857	1.768
	0.393	*0.485*	*0.375*	*0.250*	*0.395*	*0.098*	*0.053*	*0.137*	*0.157*			*0.254*	*0.160*	*0.216*	*0.264*

[a] For hydrates with a single type of metal atom, M2 = M1. [b] Electron density (e Å^{-3}) at bond critical points given in italics.

109.47°) are less stable than the nontetrahedral ones by 1.2 and 0.5 kcal mol^{-1}, respectively.

The entries in italics listed in Table 2 and Table 3 indicate the values of the electron density $\rho(\mathbf{r}_c)$ at bond critical points (BCPs), obtained with AIM2000.[26] The magnitude of $\rho(\mathbf{r}_c)$ depends on interatomic distance and the degree of coordination of the atoms and is often used as a measure of the bond strength for similar types of bonds.[26,27] For example, in the two-coordinate hydrate $[Cu(H_2O)_2(H_2O)_2]^+$ the Cu−O distances are shorter than in three-coordinate $[Cu(H_2O)_3(H_2O)]^+$; three-coordinate $[Cu(H_2O)_3(H_2O)]^+$ has shorter Cu−O bonds than four-coordinate $[Cu(H_2O)_4]^+$, except for the Cu1−O1 bond. As expected, the values of $\rho(\mathbf{r}_c)$ for Cu−O bonds are highest for two-coordinate $[Cu(H_2O)_2(H_2O)_2]^+$ and decrease in $[Cu(H_2O)_3(H_2O)]^+$ and $[Cu(H_2O)_4]^+$. Similar results were obtained for the Ag^+ hydrates $[Ag(H_2O)_2(H_2O)_2]^+$, $[Ag(H_2O)_3(H_2O)]^+$, and $[Ag(H_2O)_4]^+$.

In comparing analogous hydrates of Cu^+ and Ag^+ it is seen that the Cu−O interatomic distances are shorter than Ag−O ones. For example, in two-coordinate $[Cu(H_2O)_2(H_2O)_2]^+$ the Cu−O distance is 1.876 Å whereas in $[Ag(H_2O)_2(H_2O)_2]^+$ Ag−O distance is 2.206 Å. Shorter M−O bonds are also seen in three-coordinate $[Cu(H_2O)_3(H_2O)]^+$ relative to $[Ag(H_2O)_3(H_2O)]^+$, and in four-coordinate $[Cu(H_2O)_4]^+$ relative to $[Ag(H_2O)_4]^+$. At the same time, the values of $\rho(\mathbf{r}_c)$ are larger for Cu−O than for Ag−O bonds, a further indication that Cu−O bonds are stronger the Ag−O analogues (Table 2). For example the value of $\rho(\mathbf{r}_c)$ for Cu−O bonds in $[Cu(H_2O)_2(H_2O)_2]^+$ is 0.658 e Å^{-3} whereas that for Ag−O bonds in $[Ag(H_2O)_2(H_2O)_2]^+$ it is 0.422 e Å^{-3}. These results are consistent with the fact that the dissociation energies of the diatomics CuO and AgO are 64.3 ± 3.5 and 52.7± 3.5 kcal mol^{-1}, respectively.[16]

Three structures were found initially for the Cu^+ and Ag^+ hydrates involving six water molecules. The Cu^+ species, showing the covalent bonds, are displayed in Figure 2a,c,e. The molecular graphs obtained with AIM2000 are displayed as Figure 2b,d,f. As seen in the case of the four-water hydrates, $[Cu(H_2O)_2(H_2O)_4]^+$ has only two water molecules in the first shell (Figure 2a). The other four water molecules interact with the first shell through hydrogen bonds. In the case of $[Cu(H_2O)_4(H_2O)_2]^+$ (Figure 2b) four water molecules are included in the first shell and the other two make up the second shell. As seen in the case of the four-water hydrates, the Cu−O distances are shorter and the values of $\rho(\mathbf{r}_c)$ are larger in two-coordinate $[Cu(H_2O)_2(H_2O)_4]^+$ than in four-coordinate $[Cu(H_2O)_4(H_2O)_2]^+$. Not surprisingly, the Cu−O distances and the values of $\rho(\mathbf{r}_c)$ for the first shell of $[Cu(H_2O)_2(H_2O)_2]$ are very close to the values for the first shell of $[Cu(H_2O)_2(H_2O)_4]$. As reported by Curtiss,[14] we obtained a third six-water hydrate, six-coordinate $[Cu(H_2O)_6]^+$ (Figure 2c), when the default convergence criteria were used in the optimizations. Analogous six-water hydrates $[Ag(H_2O)_2(H_2O)_4]^+$, $[Ag(H_2O)_4(H_2O)_2]^+$, and $[Ag(H_2O)_6]^+$ were found for Ag^+. Similar bonding patterns were found for these hydrates as in the case of the Cu^+ species. The molecular graphs of the Ag^+ analogues are included in Supplementary Figure 1 as (d), (e), and (f), respectively. However, frequency analyses on the optimized geometries obtained with the default convergence criteria yielded 10 and 8 imaginary frequencies for six-coordinate $[Cu(H_2O)_6]^+$ and $[Ag(H_2O)_6]^+$, respectively. On the other hand no imaginary frequencies were obtained for $[Cu(H_2O)_2(H_2O)_2]^+$, $[Cu(H_2O)_3(H_2O)]^+$, $[Cu(H_2O)_4]^+$, $[Cu(H_2O)_2(H_2O)_4]^+$, $[Cu(H_2O)_4(H_2O)_2]^+$ and their Ag^+ analogues. Schmiedekamp and co-workers[28] also reported that six-coordinate $[Co(H_2O)_6]^{2+}$ exhibits a large number of imaginary frequencies. In our case, the lowest imaginary-frequency modes corresponded to movement of the axial water molecules. The imaginary frequencies—several were lower than 200 cm^{-1}—were not small, an indication that lower energy structures were available. Indeed, when $[Cu(H_2O)_6]^+$ and $[Ag(H_2O)_6]^+$ were re-optimized with tighter convergence criteria (Opt=Tight), two water molecules moved from the first shell into second shell with formation of $[Cu(H_2O)_4(H_2O)_2]^+$ and $[Ag(H_2O)_4(H_2O)_2]^+$, respectively. It is clear that the six-coordinate hydrates $[Cu(H_2O)_6]^+$ and $[Ag(H_2O)_6]^+$ are not minima on the potential energy surface in the gas phase. As far as the molecular structure (bonding) is concerned, in the case of $[Cu(H_2O)_6]^+$ the axial Cu−O bonds (Cu−O1, Cu−O2) are shorter than the four equatorial Cu−O bonds and the values of $\rho(\mathbf{r}_c)$ are significantly larger (0.436 e Å^{-3}) than the values for the equatorial bonds (0.192 and 0.153 e Å^{-3}). The axial bonds of $[Cu(H_2O)_6]^+$ are shorter and stronger than the Cu−O bonds of $[Cu(H_2O)_4(H_2O)_2]^+$ that exhibit $\rho(\mathbf{r}_c)$ values of 0.380 e Å^{-3}. These features are also seen in the Ag^+ analogues.

Structure of CuS^- and AgS^- Hydrates. We began the optimization of the $[MS(H_2O)_4]^-$ complexes with three water

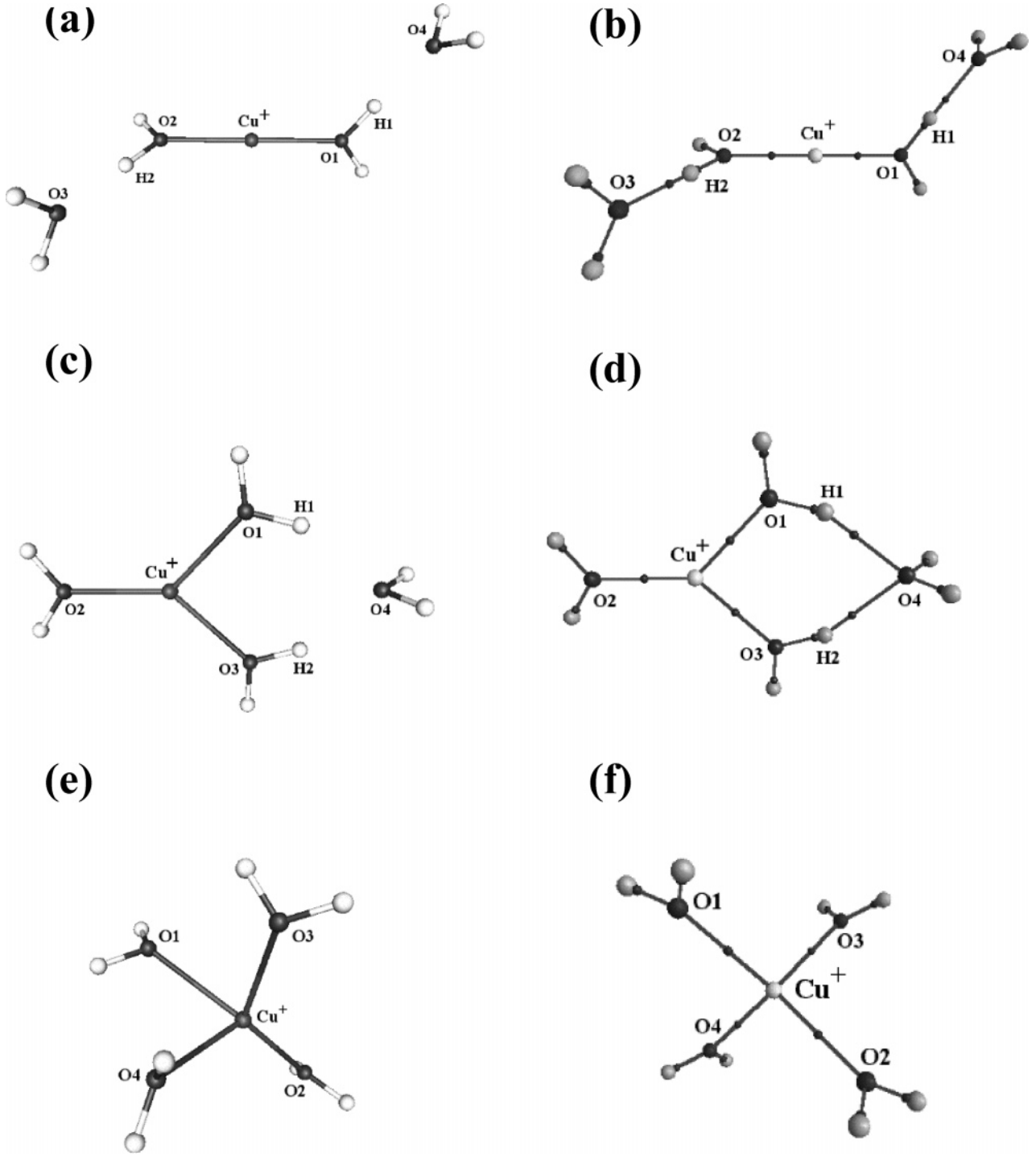

Figure 1. Displays of (a) $[Cu(H_2O)_2(H_2O)_2]^+$ showing covalent Cu−O bonds, (b) the complete molecular graph of $[Cu(H_2O)_2(H_2O)_2]^+$ with small black spheres indicating bond critical points, (c) $[Cu(H_2O)_3(H_2O)]^+$ showing covalent Cu−O bonds, (d) the complete molecular graph of $[Cu(H_2O)_3(H_2O)]^+$ with small spheres indicating bond critical points, (e) $[Cu(H_2O)_4]^+$ showing covalent Cu−O bonds, and (f) the complete molecular graph of $[Cu(H_2O)_4]^+$ with small spheres indicating bond critical points.

molecules positioned around the metal and one water molecule placed adjacent to sulfur but only one H_2O remained bonded directly to the metal atom. The two other water molecules moved from the metal toward the sulfur atom. The $[CuS(H_2O)_4]^-$ hydrate showing the Cu−O and Cu−S covalent bonds is displayed in Figure 3a and its molecular graph is shown as Figure 3b. The molecular graph of $[AgS(H_2O)_4]^-$ is included in Supplementary Figure 2 as (a). $[CuS(H_2O)_4]^-$ and $[AgS(H_2O)_4]^-$ exhibit similar molecular graphs and have only a single H_2O bonded to the metal; two water molecules, identified through O2 and O3 are hydrogen bonded to sulfur. The fourth water molecule (O4) not directly connected to MS^- forms three hydrogen bonds (O2−H4, O3−H3, and O4−H1) with the three first-shell water molecules yielding a bicyclic structure. On the basis of the values of $\rho(\mathbf{r}_c)$ and interatomic distances, the S−H hydrogen bonds are relatively weak. The key first-solvation-shell interaction in the case of $[CuS(H_2O)_4]^-$ and $[AgS(H_2O)_4]^-$ involves the formation of only one M−O bond. The values of $\rho(\mathbf{r}_c)$ for Cu−S and Ag−S bonds are 0.699 and 0.516 e Å^{-3}, respectively, an indication that Cu−S bonds are stronger than Ag−S bonds. This is also the case for Cu−O (0.480 e Å^{-3}) and Ag−O (0.304 e Å^{-3}) bonds. Generally speaking, the

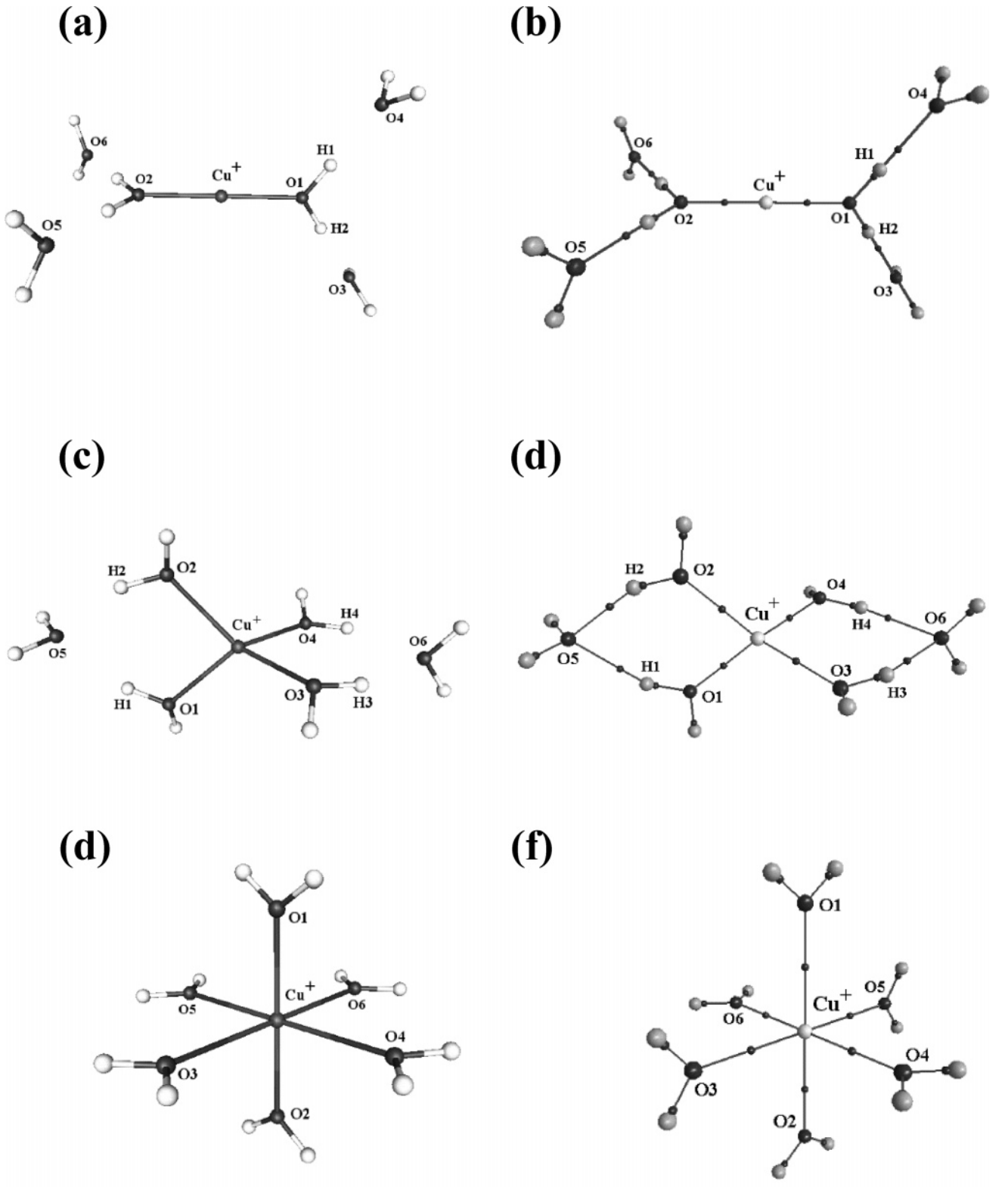

FIG. 2

Figure 2. Displays of (a) $[Cu(H_2O)_2(H_2O)_4]^+$ showing covalent Cu−O bonds, (b) the complete molecular graph of $[Cu(H_2O)_2(H_2O)_4]^+$ with small spheres indicating bond critical points, (c) $[Cu(H_2O)_4(H_2O)_2]^+$ showing covalent Cu−O bonds, (d) the complete molecular graph of $[Cu(H_2O)_4(H_2O)_2]^+$ with small spheres indicating bond critical points, (e) $[Cu(H_2O)_6]^+$ showing covalent Cu−O bonds, and (f) the complete molecular graph of $[Cu(H_2O)_6]^+$ with small spheres indicating bond critical points.

interactions of solute with solvent in hydration of CuS^- and AgS^- are comparable.

In the case of the $[MS(H_2O)_6]^-$ hydrates, we began with five molecules arranged around the metal, and one water molecule positioned near sulfur. As was seen in the case of the $[MS(H^2O)_4]^-$ species, optimization yielded structures in which only one H_2O remained covalently bonded to the metal atom. For $[CuS(H_2O)_6]^-$, Figure 3c shows only the Cu−S and Cu−O covalent bonds and Figure 3d is its molecular graph; the molecular graph of $[AgS(H_2O)_6]^-$ is included in Supplementary Figure 2 as (b). One portion of the hydrate involving four water molecules is virtually identical to $[CuS(H_2O)_4]^-$. The other two

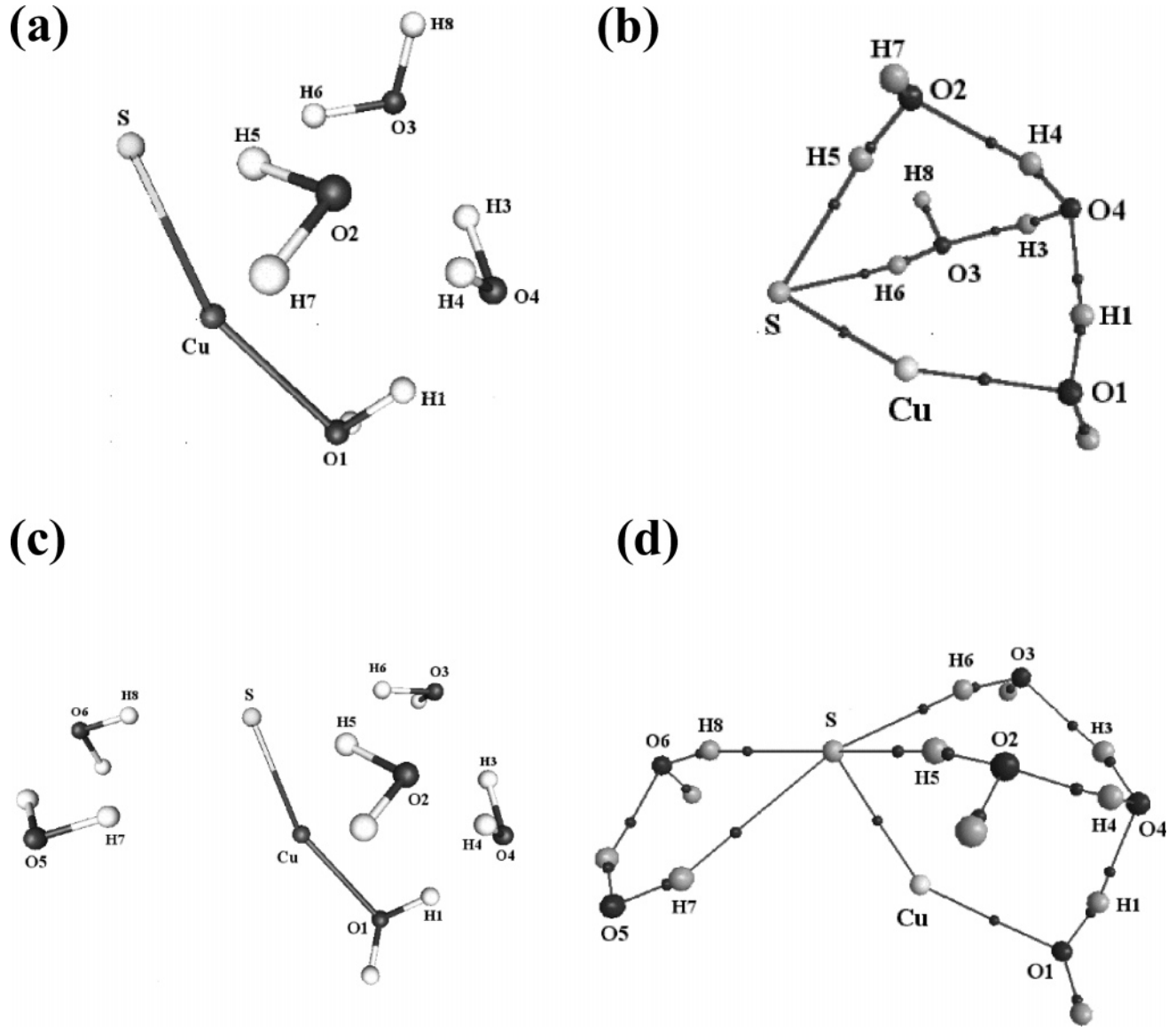

Figure 3. Displays of (a) $[CuS(H_2O)_4]^-$ showing covalent Cu−S and Cu−O bonds, (b) the complete molecular graph of $[CuS(H_2O)_4]^-$ with small spheres indicating bond critical points, (c) $[CuS(H_2O)_6]^-$ showing covalent Cu−S and Cu−O bonds, and (d) the complete molecular graph of $[CuS(H_2O)_4]^-$ with small spheres indicating bond critical points.

water molecules that hydrogen bond to each other, move and form hydrogen bonds to sulfur. On the basis of interatomic distances and values of $\rho(\mathbf{r}_c)$, the M−S and M−O bonds in the $[MS(H_2O)_6]^-$ hydrates are similar in strength to comparable bonds of the $[MS(H_2O)_4]^-$ hydrates. Vibration analyses on the optimized geometries of $CuS(H_2O)_4]^-$ and $[AgS(H_2O)_4]^-$ revealed no imaginary frequencies. Remarkably, the stabilization of MS^- ions is primarily derived through inner shell solvation involving covalent bonding to only one H_2O.

Structure of Cu_2S and Ag_2S Hydrates. To model the hydration of Cu_2S and Ag_2S, we began with structures in which three water molecules were positioned around each metal atom and two water molecules near sulfur, one on each side of the molecular plane. Optimization of $[Cu_2S(H_2O)_8]$ and $[Ag_2S(H_2O)_8]$ resulted in very similar structures. Two displays of $[Cu_2S(H_2O)_8]$ are also included here. Figure 4a shows only the Cu−S and Cu−O bonds and Figure 4b is the molecular graph. The molecular graph of $[Ag_2S(H_2O)_8]$ hydrate is included in Supplementary Figure 2 as (c). In these cases, one H_2O shifted from each metal atom to the second shell—these water molecules are identified by O7 and O8 of Figure 4c—leaving each Cu coordinated to two water molecules. These two second-shell water molecules form hydrogen bonds (O7−H2 and H7−O6; O8−H3 and H8−O5) with other first-shell water molecules, two of which (O5 and O6) are hydrogen bonded to sulfur, forming a polycyclic structure. It is seen that two M−O bonds (M1−O1 and M2−O4) are slightly longer than the other two bonds M1−O2 and M2−O3. These bonds lengthen somewhat to accommodate the hydrogen bonds O6−H4 and O5−H1 to the other first-shell water molecules. On the basis of interatomic distances and values of $\rho(\mathbf{r}_c)$, it appears that hydrogen bonds between first-shell and second-shell water molecules (O7−H2 and O8−H3) are shorter and stronger than those between first-shell water molecules defined by O4 and O6 (H4−O6) and O1 and O5 (H1−O5).

Given that solvated Cu^+ and Ag^+ ions can coordinate with up to six water molecules, we searched for the structures with higher metal−water coordination by positioning five water molecules around each metal atom and two near sulfur. In this case, slightly different molecular structures were obtained for $[Cu_2S(H_2O)_{12}]$ (Figure 5a shows only the Cu−S and Cu−O bonds and Figure 5b is the molecular graph) and $[Ag_2S(H_2O)_{12}]$

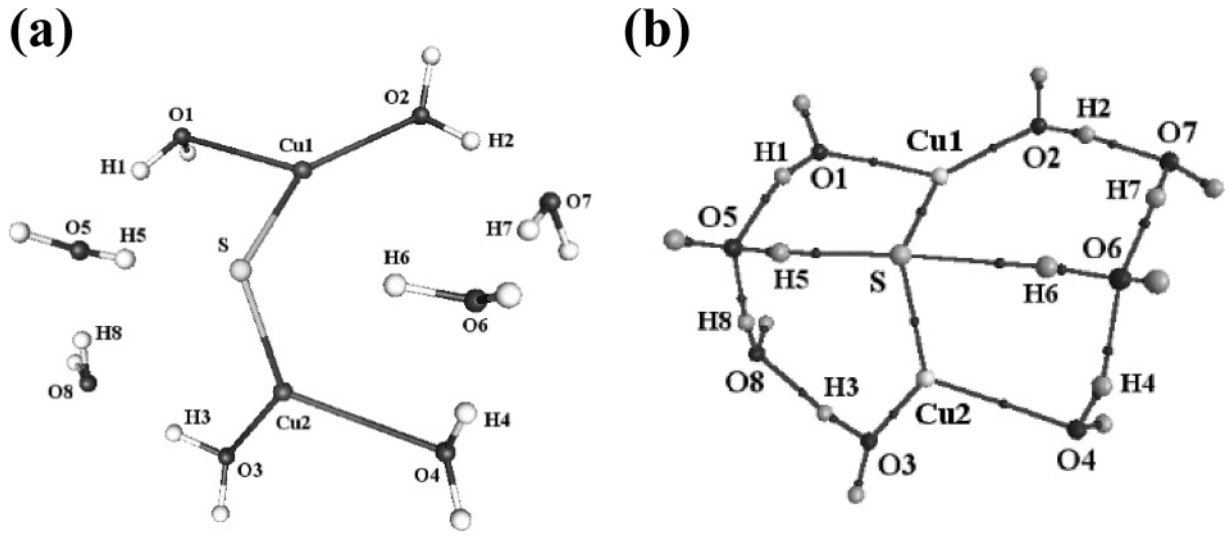

Figure 4. Displays of (a) $[Cu_2S(H_2O)_8]$ showing covalent Cu−S and Cu−O bonds and (b) the complete molecular graph of $[Cu_2S(H_2O)_8]$ with small spheres indicating bond critical points.

(Figure 5c,d). Both copper atoms of $[Cu_2S(H_2O)_{12}]$ are two-coordinate (Cu1 to O1 and O2; Cu2 to O3 and O4) whereas one of the silver atoms of $[Ag_2S(H_2O)_{12}]$ (Figure 4c) is two-coordinate (Ag1 to O1 and O2) and the other one is three-coordinate (Ag2 to O3, O4, and O10). One Cu−O bond (Cu2−O4) and two Ag−O bonds (Ag2−O4 and Ag2−O10) are considerably longer than the M1−O1, M1−O2, and M2−O3 bonds. Not unexpectedly, on the basis of the $\rho(\mathbf{r}_c)$ values, the longer Cu2−O4 bond (0.035 e Å^{-3}) is considerably weaker than other Cu−O bonds with $\rho(\mathbf{r}_c)$ ranging between 0.311 and 0.588 e Å^{-3}. Analogously, the longer Ag2−O4 (0.098 e Å^{-3}) and Ag2−O10 (0.053 e Å^{-3}) bonds are substantially weaker than the Ag1−O1(0.375 e Å^{-3}), Ag1−O2(0.250 e Å^{-3}), and Ag2−O3 (0.395 e Å^{-3}) bonds. It is interesting that no bond path was detected between Cu2 and O10 of $[Cu_2S(H_2O)_{12}]$ where the interatomic distance is 3.118 Å. On the other hand, a bond path is found between Cu2 and O4 where the interatomic distance is 3.466 Å. No meaningful differences are seen in the first shell by adding more water molecules in going from $[M_2S(H_2O)_8]$ to $[M_2S(H_2O)_{12}]$. Metal−water coordination does not change in going from $[Cu_2S(H_2O)_8]$ to $[Cu_2S(H_2O)_{12}]$ and changed only slightly in $[Ag_2S(H_2O)_{12}]$, with the formation of an additional weak Ag−O bond between Ag2 and O10. The total coordination (Cu−S and hydrogen bonds) to sulfur increased from 4 in $[M_2S(H_2O)_8]$ to 6 in $[M_2S(H_2O)_{12}]$, but the two additional hydrogen S−H bonds are weak with respect to M−S bonds on the basis of large inter-nuclear distances and the value of $\rho(\mathbf{r}_c)$ and consequently do not significantly affect complex stability. The additional four water molecules are located in the second shell.

Hydration Energies. Table 4 lists the hydration energy, E_{hyd}, which is the difference between the total energy (E_T) of the hydrate and the sum of the total energies of its components with ZPE corrections being applied to the hydrates and the components. Also included are the values $E_{hyd(uc)}$ uncorrected for basis set superposition errors (BSSEs) and the corrected values $E_{hyd(cc)}$. In our case, the BSSEs were approximated with a standard counterpoise correction (CPC) calculation. Though the BSSE is well defined for weak intermolecular interactions,[25] it is usually ignored—not defined—for strong intramolecular interactions. The $[M(H_2O)_n]^+$ complexes have covalent bonding interactions between M^+ and the H_2O molecules and the M−O inter-nuclear distances in $[M(H_2O)_2(H_2O)_2]^+$ are only slightly larger than the values found in diatomic M−O molecules. For example, the Cu−O distance of $[Cu(H_2O)_2(H_2O)_2]^+$ is 1.876 Å whereas the distance of diatomic CuO is 1.728 Å.[29] The values of $\rho(\mathbf{r}_c)$ for the Cu−O bonds of $[Cu(H_2O)_2(H_2O)_2]^+$ (0.658 e Å^{-3}) and diatomic CuO (1.097 e Å^{-3}) correlate with the bond distances. Analogously, the values of $\rho(\mathbf{r}_c)$ of the AgO bonds of $[Ag(H_2O)_2(H_2O)_2]^+$ (0.422 e Å^{-3}) and AgO (0.580 e Å^{-3}) correlate well with the bond distances that are 2.206 and 2.003 Å, respectively. Given that the Cu^+ and Ag^+ hydrates have a varying number of relatively strong covalent bonding interactions between M^+ and the H_2O molecules and weaker hydrogen bonds between water molecules, the CP corrections would be approximate at best and we expected that the BSSEs would increase with decreasing inter-nuclear separation.[30] Nevertheless, we calculated CPCs for all the complexes, keeping these points in mind. It is seen that the CPC is substantial, reaching 21.8% of the total hydration energy of $[Ag(H_2O)_6]^+$. A similar CPC of 20% was obtained for $[Cu(H_2O)_4]^+$ investigated by Feller,[10] whereas we found a CPC of 15.7%. The largest CPCs were found for the four- and six-coordinate $[M(H_2O)_n]^+$ hydrates and the smallest ones for the anionic species $[MS(H_2O)_n]^-$ that have the fewest strong M−O bonds and the largest number of hydrogen bonds. As expected, the largest CPCs were found for hydrates having the largest number of covalent M−O bonds.

It is seen that the most stable four-water hydrate of Cu^+, with or without the CPC, is two-coordinate $[Cu(H_2O)_2(H_2O)_2]^+$. Without the CPC, it is more stable than $[Cu(H_2O)_3(H_2O)]^+$ and $[Cu(H_2O)_4]^+$ by 3.9 and 9.5 kcal mol^{-1}, respectively. The differences increase to 7.8 and 16.6 kcal mol^{-1} when the CPCs are included in the hydration energies. The larger CPCs for $[Cu(H_2O)_3(H_2O)]^+$and $[Cu(H_2O)_4]^+$ are in keeping with higher metal−water coordination in these species. It appears that it is the strength of the Cu−O bonds coupled with formation of hydrogen bonds and not the degree of coordination that determines the relative stabilities of $[Cu(H_2O)_2(H_2O)_2]^+$, $[Cu(H_2O)_3(H_2O)]^+$, and $[Cu(H_2O)_4]^+$ in the gas phase. We also found the two-coordinate species $[Cu(H_2O)_2(H_2O)_4]^+$ to be the most stable six-water hydrate. Without CPCs, two-coordinate $[Cu(H_2O)_2(H_2O)_4]^+$ is lower in energy than $[Cu(H_2O)_4(H_2O)_2]^+$ and $[Cu(H_2O)_6]^+$ (not a minimum) by 8.1 and 26.2 kcal mol^{-1}, respectively. The differences increase to 15.6 and 37.0 kcal mol^{-1} when CPCs are included. Unlike the case for Cu^+, three-coordinate $[Ag(H_2O)_3(H_2O)]^+$ was found to be the most stable four-water hydrate of Ag^+—by 0.5 and 1.7.kcal mol^{-1} relative

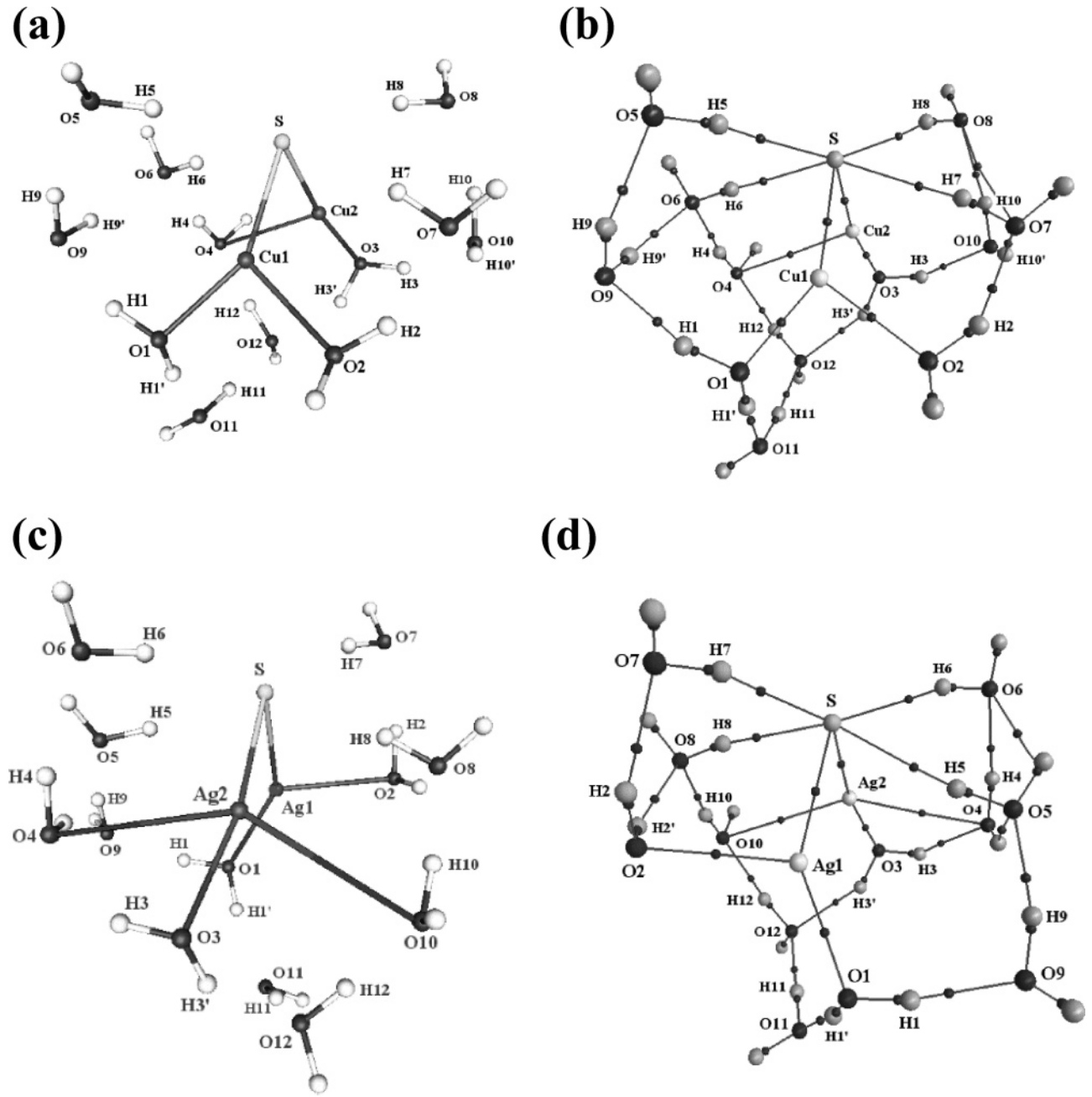

Figure 5. Displays of (a) $[Cu_2S(H_2O)_{12}]$ showing covalent Cu−S and Cu−O bonds and (b) the complete molecular graph of $[Cu_2S(H_2O)_{12}]$ with small spheres indicating bond critical points. (c) Display $[Ag_2S(H_2O)_{12}]$ showing covalent Ag−S and Cu−O bonds and (d) the complete molecular graph of $[Ag_2S(H_2O)_{12}]$ with small spheres indicating bond critical points.

to $[Ag(H_2O)_2(H_2O)_2]^+$ and $[Ag(H_2O)_4]^+$—when E_{hyd} was not CP corrected. A similar finding was reported by Feller.[10] However, when CPCs were included, two-coordinate $[Ag(H_2O)_2(H_2O)_2]^+$ was found to be more stable than $[Ag(H_2O)_3(H_2O)]^+$ and $[Ag(H_2O)_4]^+$ by 2.5 and 7.4 kcal mol^{-1}, respectively. Similar results were obtained for the six-water Ag^+ hydrates. Four-coordinate $[Ag(H_2O)_4(H_2O)_2]^+$ is more stable than $[Ag(H_2O)_2(H_2O)_4]^+$ and $[Ag(H_2O)_6]^+$ by 1.4 and 12.8 kcal mol^{-1}, respectively, when E_{hyd} is not corrected. However, when CPCs are included, two-coordinate $[Ag(H_2O)_2(H_2O)_4]^+$ was found to be more stable than $[Ag(H_2O)_4(H_2O)_2]^+$ and $[Ag(H_2O)_6]^+$ by 4.9 and 22.9 kcal mol^{-1}, respectively. We find that Cu^+ and Ag^+ have the same coordination number, unlike the observation made by Feller and co-workers.[10] In fact, we find good agreement (see column two of Table 5) between the calculated gas-phase enthalpies of hydration (ΔH_{hyd})—frequency calculations were carried out—and the experimental values for the $[Cu(H_2O)_2(H_2O)_2]^+$and $[Cu(H_2O)_3(H_2O)]^+$ pair with BSSE corrections, and the $[Ag(H_2O)_2(H_2O)_2]^+/[Ag(H_2O)_3(H_2O)]^+$ and $[Ag(H_2O)_2(H_2O)_2]^+/[Ag(H_2O)_4(H_2O)_2]^+$ pairs with BSSE corrections. Although at our level of theory it is not possible to assign preferred structures for the four-water and six-water hydrates, it is quite clear from a comparison of the calculated and experimental enthalpies of hydration ΔH_{hyd} that the species are not the four- or six-coordinate hydrates $[Cu(H_2O)_4]^+$, $[Ag(H_2O)_4]^+$, or $[Ag(H_2O)_6]^+$. Further validation of our gas-phase calculations is found in a comparison of computed enthalpies of formation for selected $[M(H_2O)_n]^+$ species in the gas phase with the values determined experimentally by collision induced dissociation (CID)[31,32] and high-pressure mass spectrometry[33] (Table 6) through a study of the process shown in eq 1. The good correlation between the calculated enthalpies of formation

TABLE 4: ZPE-Corrected Total Energies (E_T, au), Counterpoise-Uncorrected ($E_{hyd(uc)}$), and Counterpoise-Corrected Hydration Energies ($E_{hyd(cc)}$, kcal mol^{-1})

species	E_T	$E_{hyd(cu)}$	$E_{hyd(cc)}$
Cu^+	−1640.136904		
CuS^-	−2038.675334		
Cu_2S	−3679.131012		
H_2O	−76.391540		
$[Cu(H_2O)_2(H_2O)_2]+$	−1945.892230	−118.7	−111.0 (6.9%)
$[Cu(H_2O)_3(H_2O)]+$	−1945.886031	−114.8	−103.2 (11.2%)
$[Cu(H_2O)_4]+$	−1945.877093	−109.2	−94.4 (15.7%)
$[Cu(H_2O)_2(H_2O)_4]^+$	−2098.717384	−145.2	−137.6 (5.5%)
$[Cu(H_2O)_4(H_2O)_2]^+$	−2098.704553	−137.1	−122.6 (11.3%)
$[Cu(H_2O)_6]+$	−2098.675913	−119.0	−100.6 (18.3%)
$[CuS\ (H_2O)_4]^-$	−2344.344064	−64.3	−60.7 (5.9%)
$[CuS\ (H_2O)_6]^-$	−2497.163354	−87.1	−82.4 (5.7%)
$[Cu_2S(H_2O)_8]$	−4290.433677	−106.9	−96.5 (10.8%)
$[Cu_2S(H_2O)_{12}]$	−4596.063533	−146.9	−136.7 (6.0%)
Ag^+	−5199.258847		
AgS^-	−5597.743002		
Ag_2S	−10797.277817		
AgCuS	−7238.204993		
$[Ag(H_2O)_2(H_2O)_2]+$	−5504.962057	−86.0	−80.1 (7.4%)
$[Ag(H_2O)_3(H_2O)]+$	−5504.962889	−86.5	−77.6 (11.5%)
$[Ag\ (H_2O)_4]+$	−5504.960104	−84.8	−72.7 (16.6%)
$[Ag(H_2O)_2(H_2O)_4]^+$	−5657.782278	−109.3	−103.3 (5.8%)
$[Ag(H_2O)_4(H_2O)_2]^+$	−5657.784488	−110.7	−98.4 (12.5%)
$[Ag\ (H_2O)_6]+$	−5657.764200	−97.9	−80.4 (21.8%)
$[AgS\ (H_2O)_4]^-$	−5903.404640	−59.9	−56.5 (6.0%)
$[AgS\ (H_2O)_6]^-$	−6056.224563	−83.1	−78.4 (6.0%)
$[Ag_2S(H_2O)_8]$	−11408.564516	−96.9	−86.2 (12.4%)
$[Ag_2S(H_2O)_{12}]$	−11714.189256	−133.6	−123.4 (8.3%)
$[AgCuS(H_2O)_8]$	−7849.499909	−102.0	

TABLE 5: Enthalpy of Formation (ΔH_{hyd}) and Solvent-Field Energy (ΔE_{sf}) of Hydrates (kcal mol^{-1})

hydrate	ΔH_{hyd}	ΔE_{sf}	$(\Delta H_{hyd} + \Delta E_{sf})$
$[Cu(H_2O)_2(H_2O)_2]^+$	113.5 (*121.2*)[a]	53.4	166.9
	106.0 ± 3.0[b]		
$[Cu(H_2O)_3(H_2O)]^+$	105.6 (*117.2*)	62.4	168.0
$[Cu^+(H_2O)_4]^+$	98.2 (*113.0*)	68.1	166.3
			145.1[d]
$[Cu(H_2O)_2(H_2O)_4]^+$	140.3	47.9	188.2
$[Cu(H_2O)_4(H_2O)_2]^+$	126.1	57.7	183.8
$[Cu^+(H_2O)_6]^+$	105.5	83.5	189.0
$[CuS\ (H_2O)_4]^-$	64.5	66.1	110.6
$[CuS\ (H_2O)_6]^-$	86.8	61.2	148.0
$[Cu_2S(H_2O)_8]$	102.8	30.9	133.7
$[Cu_2S(H_2O)_{12}]$	145.7	45.3	191.0
$[Ag(H_2O)_2(H_2O)_2]^+$	82.1 (*88.0*)	54.5	136.6
	88.6± 2.2[c]		
$[Ag(H_2O)_3(H_2O)]^+$	79.8 (*88.7*)	60.8	140.6
$[Ag(H_2O)_4]^+$	74.0 (*86.0*)	69.9	143.9
			116.6[d]
$[Ag\ (H_2O)_2(H_2O)_4]^+$	105.8 (*111.7*)	51.0	156.8
	115 ± 2.2[c]		
$[Ag\ (H_2O)_4(H_2O)_2]^+$	101.2 (*113.5*)	59.9	161.1
$[Ag(H_2O)_6]^+$	84.0 (*101.5*)	83.9	167.9
$[AgS(H_2O)_4]^-$	60.1	65.9	126.0
$[AgS\ (H_2O)_6]^-$	83.0	61.1	144.1
$[Ag_2S(H_2O)_8]$	91.7	32.4	124.1
$[Ag_2S(H_2O)_{12}]$	131.9	27.1	159.0

[a] Values in italics in parentheses do not include the BSSE corrections. [b] Experimental values from refs 32 and 33. [c] Experimental values from ref 31. [d] Experimental values from re 37.

and the experimental values also indicates that hydrogen bonds in these species are

$$[M(H_2O)_n]^+ \rightarrow [M(H_2O)_{n-1}]^+ + H_2O \qquad (1)$$

modeled reliably at the level of theory used in this study. The difference between calculated and experimental enthalpies observed in going from $[Cu(H_2O)_4]^+$ to $[Cu(H_2O)_3]^+$ ($\Delta H_{4,3}$) and from $[Cu(H_2O)_3]^+$ to $[Cu(H_2O)_2]^+$ ($\Delta H_{3,2}$) is acceptable given the variations in the experimental data. For example, whereas Dalleska[12] reported 12.8 kcal mol^{-1} for $\Delta H_{4,3}$, Holland[31] found a value of 16.7 kcal mol^{-1}. We calculated 17.5 kcal mol^{-1} for $\Delta H_{4,3}$. A similar situation is seen in the case of $\Delta H_{3,2}$; Dalleska[12] and Magnera[32,33] reported 13.7 and 17.0 kcal mol^{-1}, respectively, and we calculated a value of 18.7 kcal mol^{-1}. The remaining calculated values of $\Delta H_{n,n-1}$ for both Cu^+ and Ag^+ correlate well with the experimental data.

TABLE 6: Calculated and Experimental Enthalpies of Dissociation of Metal−Cation Hydrates at 298 K

$[M(H_2O)_n]^+$	n to $n-1$	calcd $\Delta H_{n,n-1}$	exp $\Delta H_{n,n-1}$
Cu	6, 5	13.0	
	5, 4	13.8	14.0[a]
	4, 3	17.5	12.8[b]
	3, 2	18.7	13.7[b]
	2, 1	38.0	40.7[b]
	1, 0	39.3	38.4[b]
Ag	6, 5	11.5	13.3[a]
	5, 4	12.2	13.7[a]
	4, 3	15.3	14.9[a]
	3, 2	16.1	15.0[a]
	2, 1	24.5	25.4[a]
	1, 0	26.2	33.3[a]

[a] Experimental values from ref 31. [b] Experimental values from ref 12.

However, it is possible that the relative stabilities of the hydrates in aqueous solution differ from the gas phase so solvent field calculations could shed light on this possibility.In fact, in an investigation of aqueous solutions of $AgNO_3$ and $AgClO_4$ with extended X-ray absorption fine structure (EXAFS) spectroscopy, Seward[34] and Yamaguchi[35] found hydrated Ag^+ to be a four-coordinate species, presumably the structure displayed as Figure 1e. They also found that the coordination of Ag^+ decreased from four to three when the temperature was increased from 25 to 350 °C. Concomitantly, the Ag−O interatomic distance decreased by 0.1 Å. In fact, our calculations also predict a decrease of ∼0.1 Å in the Ag−O distance from ∼2.4 to ∼2.3 Å (see Table 2) in going from four-coordinate $[Ag(H_2O)_4]^+$ to three-coordinate $[Ag(H_2O)_3(H_2O)]^+$. A phase transition from liquid to equilibrium-saturated vapor accompanied the change of the temperature from 25 to 350 °C. This result suggests that a further transition from equilibrium-saturated vapor to the gaseous phase might decrease the Ag^+ coordination from three to two.

Though the CP corrected hydration energies for $[Cu(H_2O)_2(H_2O)_2]^+$ and $[Cu(H_2O)_2(H_2O)_4]^+$ are significantly greater (by 30.9 and 34.3 kcal mol^{-1}) than the corresponding values for $[Ag(H_2O)_2(H_2O)_2]^+$ and $[Ag(H_2O)_2(H_2O)_4]^+$, the hydration energy of $[CuS(H_2O)_4]^-$ is only marginally larger (uncorrected by 4.4, corrected by 4.2 kcal mol^{-1}) than the energy for $[AgS(H_2O)_4]^-$. For $[CuS(H_2O)_6]^-$, E_{hyd} is higher than the value for $[AgS(H_2O)_6]^-$ by 4.0 kcal mol^{-1} uncorrected and 4.0 kcal mol^{-1} corrected. The hydration energies of $[Cu_2S(H_2O)_8]$ are larger than the Ag^+ analogues $[Ag_2S(H_2O)_8]$; 10.0 kcal mol^{-1} uncorrected and 10.3 kcal mol^{-1} corrected. The differences in E_{hyd} between $[Cu_2S(H_2O)_{12}]$ and $[Ag_2S(H_2O)_{12}]$ are 13.3 kcal mol^{-1} uncorrected and 13.3 kcal mol^{-1} corrected in favor of the copper complex. That the hydration energies of Cu^+, CuS^-, and Cu_2S are higher than the values for Ag^+, AgS^-, and Ag_2S is explained by he fact that the Cu−O bonds are stronger than Ag−O bonds when the coordination to the metal is identical.

Solvent Field Calculations. In columns two and three of Table 5 are listed CP corrected ΔH_{hyd} and ΔE_{sf}, that is the energy for embedding the hydrates in the water solvent field of dielectric constant 78. Calculated as the difference between E_T of the hydrate in the gas phase and the E_T of the hydrate in the solvent field, ΔE_{sf} simulates the polar effect of the bulk solution. Like the gas-phase hydration energies, the solvent-field hydration energies of Cu^+ and its sulfides are higher than the values for the corresponding Ag^+ and AgS species. For pairs of hydrates with the same net charge and size, the ΔE_{sf} values, perhaps not surprisingly, are virtually identical. Fo example, the ΔE_{sf} values for $[Cu(H_2O)_2(H_2O)_2]^+$ and $[Ag(H_2O)_2(H_2O)_2]^+$ are 53.4 and 54.5 kcal mol^{-1}, respectively. Similar results are found for the $[Cu(H_2O)_4]^+$ and $[Ag(H_2O)_4]^+$ pair, the $[Cu(H_2O)_6]^+$ and $[Ag(H_2O)_6]^+$ pair, the $[CuS(H_2O)_n]^-$ and $[AgS(H_2O)_n]^-$ pair, and the $[Cu_2S(H_2O)_8]$ and $[Ag_2S(H_2O)_8]$ pair. However, the $[Cu_2S(H_2O)_{12}]$ and $[Ag_2S(H_2O)_{12}]$ complexes with slightly different structures and metal−water coordination, exhibit significantly different values of 45.3 and 27.1 kcal mol^{-1}, respectively. The ΔE_{sf} for the neutral hydrates $[M_2S(H_2O)_n]$ is only one-half the value of ΔE_{sf} for charged species $[M(H_2O)_n]^+$ and $[MS(H_2O)_n]^-$. The contribution of ΔE_{sf} in the case of neutral $[M_2S(H_2O)_n]$ species is less than 22% of the total hydration energy so the difference in these values for $[Cu_2S(H_2O)_{12}]$ and $[Ag_2S(H_2O)_{12}]$ has a minimal effect in determining their relative total energies in a solvent field.

We also carried out an analysis of the sum of ΔH_{hyd}, and solvent-field energy ΔE_{sf} ($\Delta H_{hyd} + \Delta E_{sf}$), the values being collected in column 4 of Table 5. To compare calculated and experimental values of ΔH, in principle, full optimizations and frequency analyses of the hydrates embedded in the solvent field should be performed and ΔH_{sf} obtained. However, given the magnitude of this task for all the hydrates and that fact that the electronic energy is the main determinant of the enthalpy of formation of the hydrates, we assumed that the geometrical parameters and zero point energies of the hydrates in the solvent field would not differ significantly from the gas phase values. To validate this assumption, we optimized only $[Cu(H_2O)_4]^+$ in the water solvent field with SCI-PCM. As expected, the geometries differed only marginally and the ZPE and thermal corrections to the enthalpy decreased only by 2.7 and 2.9 kcal mol^{-1}, respectively, in the solvent field relative to the gas phase. These values are small compared to the change in electronic energy (ΔE_{sf} = 68.1 kcal mol^{-1}) in going from the gas phase to the solvent field. Consequently, our assumptions that ΔH_{sf}, $\cong \Delta E_{sf}$, and that it is not necessary to optimize the hydrates in the solvent field are justified. It is seen that the sum ($\Delta H_{hyd} + \Delta E_{sf}$) is considerably larger than experimental values.[36] For the tetra-hydrate species $[Cu(H_2O)_4]^+$ and $[Ag(H_2O)_4]^+$ the differences between the computed and experimental values are 21.2 and 27.3 kcal mol^{-1}, respectively. Of importance is the fact that there is a remarkable leveling of the relative stabilities when the hydrates are imbedded in the polar water solvent field. In the case of the four-water hydrates all three species exhibit virtually identical stabilities. The same result is seen in the case of the six-water hydrates. Of course, these calculations do not include differences in the energies of cavity formation which may favor the more symmetrical species $[Cu(H_2O)_4]^+$ and $[Cu(H_2O)_6]^+$. Although the two-coordinate hydrates are calculated to be the most stable in the gas phase, the leveling effect of the solvent field indicates that the four coordination may be preferred in aqueous solution for $[M(H_2O)_4]^+$, nicely in keeping with experimental results obtained by Seward,[34] Yamaguchi,[35] and Ohtaki.[37]

Inclusion of more water molecules in the first and second shell, as in $[M(H_2O)_2(H_2O)_4]^+$, $[M(H_2O)_4(H_2O)_2]^+$, and $[M(H_2O)_6]^+$ worsens the correlation between the calculated and experimental hydration enthalpies. For example the calculated value ($\Delta H_{hyd} + \Delta E_{sf}$) for $[Cu(H_2O)_4(H_2O)_2]^+$ was 183.8 kcal mol^{-1} whereas the experimental value was only 145.1 kcal mol^{-1}. Analogously the value of ($\Delta H_{hyd} + \Delta E_{sf}$) for $[Ag(H_2O)_4(H_2O)_2]^+$ was 161.1 kcal mol^{-1} whereas experimental value was 116.6 kcal mol^{-1}. In a theoretical investigation of hydrated Ag^+, Martinez and co-workers[13] also observed that the inclusion of second and third shells of water molecules worsened the convergence between calculated and experimental enthalpies of hydration of Ag^+.[13] Sanchez[38] and Jain[39] also have commented on the overestimation of enthalpies of hydration obtained computationally. Accurate calculations of hydration must include the enthalpy of formation of the cavity in the solvent, ΔH_{cav}, the enthalpy of vaporization of water, ΔH_{vap}, and ΔH_{disp}, the enthalpy that accounts for dispersion-repulsion forces between solvent and solute.[40] Daleska and co-workers[12] showed that inclusion of these corrections, calculated by empirical formulas,[41,42] improves the accuracy somewhat but the error in the hydration enthalpy remains high, up to 31 kcal mol^{-1}. The largest source of discrepancy between calculated and experimental values is still not totally resolved due to the number of factors involved. Consequently, we chose not to include empirical approximations in our analysis.

Our calculations also allowed us to model the gas phase and solution phase ionic dissociation reactions of Cu_2S and Ag_2S.

$$Cu_2S \rightarrow Cu^+ + CuS^- \qquad \Delta E_T = 200.0 \text{ kcal mol}^{-1} \quad (2)$$

$$Ag_2S \rightarrow Ag^+ + AgS^- \qquad \Delta E_T = 173.2 \text{ kcal mol}^{-1} \quad (3)$$

On the basis of the data collected in Table 4, the dissociation energies of the hydrates including only the important first shell hydration are shown in

$$[Cu_2S(H_2O)_8]_g \rightarrow [Cu(H_2O)_2(H_2O)_2]^+_g + [CuS(H_2O)_4]^-_g \qquad \Delta E_T = 123.9 \text{ kcal mol}^{-1} \quad (4)$$

$$[Ag_2S(H_2O)_8]_g \rightarrow [Ag(H_2O)_2(H_2O)_2]^+_g + [AgS(H_2O)_4]^-_g \qquad \Delta E_T = 124.1 \text{ kcal mol}^{-1} \quad (5)$$

The inclusion of explicit first-shell hydration substantially reduces the endothermicity of the reactions. Of interest is the fact that the difference between Cu_2S and Ag_2S is reduced to 0.2 kcal mol^{-1}, undoubtedly because Cu^+ exhibits a higher hydration energy than Ag^+. Although there is a lower degree of coordination of metal atoms in the products $[M(H_2O)_2(H_2O)_2]^+$ and $[MS(H_2O)_4]^-$ with respect to $[M_2S(H_2O)_8$, the M−O bonds of $[M(H_2O)_2(H_2O)_2]^+$ are stronger than the M−O bonds of in $[M_2S(H_2O)_8]$, as reflected in shorter bond distances and higher values of $\rho(\mathbf{r}_c)$ (Table 2). The dissociation energies decreased further when the hydrates were embedded in a solvent field because of the differential electrostatic stabilization of the charged species. As seen in eq 5 and eq 6, enormous decreases of over 100 kcal mol^{-1} are realized in the dissociation energies.

$$[Cu_2S(H_2O)_8]_{sf} \rightarrow [Cu(H_2O)_4]^+_{sf} + [CuS(H_2O)_4]^-_{sf} \qquad \Delta E_T = 32.6 \text{ kcal mol}^{-1} \quad (6)$$

$$[Ag_2S(H_2O)_8]_{sf} \rightarrow [Ag(H_2O)_4]^+_{sf} + [AgS(H_2O)_4]^-_{sf} \qquad \Delta E_T = 25.5 \text{ kcal mol}^{-1} \quad (7)$$

Metal Substitution. In this context, we explored the substitution of Cu^+ by Ag^+ in Cu_2S, the motivation being the facile displacement of Cu(II) by Ag(I) in solution reported by Kraus and co-workers.[18] We began our substitution studies with Cu_2S and Ag(I) before proceeding to the Cu(II)−Ag(I) reaction. The results are summarized in

$$Ag^+ + Cu_2S \rightarrow Cu^+ + AgCuS \quad \Delta E = 30.1 \text{ kcal mol}^{-1} \quad (8)$$

$$[Ag(H_2O)_4]^+ + [Cu_2S(H_2O)_8] \rightarrow [Cu(H_2O)_4]^+ + [AgCuS(H_2O)_8] \; \Delta E = 10.5 \text{ kcal mol}^{-1} \quad (9)$$

The endothermicity of reaction shown in eq 8 for the gas-phase results from the replacement of a Cu−S bond with a weaker Ag−S bond. The molecular structures of AgCuS and its first-shell hydrate $[AgCuS(H_2O)_8]$ are very similar to those of Cu_2S and $[Cu_2S(H_2O)_8]$. The corresponding geometrical parameters, values of $\rho(\mathbf{r}_c)$, and E_T's are given in Table 2 and Table 3. Despite the substantial decrease of ΔE_T from 30.3 to 10.5 kcal mol^{-1} seen upon the addition of the first hydration shell, the substitution reaction remains endothermic basically because a Cu−S bond is replaced by a weaker Ag−S bond even though the hydration energy of Cu^+ is significantly larger than it is for Ag^+.

Conclusions

Hydration of Cu(I) and Ag(I), CuS^-, AgS^-, Cu_2S, Ag_2S was modeled by explicit ab initio and solvent field methods yielding molecular structures of first- and second-shell species. The hydration energy contributes more to the total solvation energy of hydrated cations Cu^+, Ag^+ and molecules Cu_2S, Ag_2S than to that of anions CuS^- and AgS^- because of higher coordination of metal atoms in the former case. The solvent-field energy, that simulates long range polar interactions, was found to be approximately equal for Cu^+, Ag^+, their sulfides CuS^-, AgS^-, but substantially larger than that for hydrated neutral molecules Cu_2S and Ag_2S. The experimentally measured coordination and enthalpy of formation of hydrated copper and silver cations are predicted computationally with excellent accuracy. Our calculations predict the Cu_2S to be more stable than Ag_2S both in gas phase and in aqueous solution. At the same time, our calculations are not sufficiently accurate to describe the small differences in experimental values of free energies of solvated Cu_2S and Ag_2S due to the number of undetermined factors. The dissociation and substitution reactions of metal sulfides in gas and in solution were compared. The decrease of energy of reactions going from gas to solution is explained on the basis of coordination of metal atoms to water molecules and changes in bond strengths in the first hydration shell.

Acknowledgment. We thank SHARCNET (Shared Hierarchical Academic Research Computing Network (of Ontario)) for providing computing resources at McMaster University and a Postdoctoral Fellowship (in part) for B.N. We gratefully acknowledge financial support by the Natural Sciences and Engineering Research Council of Canada.

Supporting Information Available: Molecular graphs. This material is available free of charge via the Internet at http://pubs.acs.org.

References and Notes

(1) Rees, D. C. *Annu. Rev. Biochem.* **2002**, *71*, 221.
(2) Alvarez, M. L.; Ai, J.; Zumft, W.; Sanders-Loehr, J.; Dooley, D. M. *J. Am. Chem. Soc.* **2001**, *123*, 576.
(3) Rasmussen, T.; Berks, B. C.; Sanders-Loehr, J.; Dooley, D. M.; Zumft, W. G.; Thomson, A. J. *Biochemistry* **2000**, *39*, 12753.
(4) Hogstrand C.; Wood C. M. *Environ. Toxicol. Chem.* **1998**, *17*, 547.
(5) Wood C. M.; Playle R. C.; Hogstrand C. *Environ. Toxicol. Chem.* **1999**, *18*, 71.
(6) Brix, K. V.; DeForest, D. K.; Adams, W. J. *Environ. Toxicol. Chem.* **2001**, *20*, 1846.
(7) Huebert, D. B.; Dyck, B. S.; Shay, J. M. *Aquatic Toxicol.* **1993**, *24*, 183.
(8) Bianchini, A.; Bowles, K. C.; Brauner, C. J.; Gorsuch, J. W.; Kramer, J. R.; Wood, C. M. *Environ. Toxicol. Chem.* **2002**, *21*, 1294.
(9) Ogden N. L.; Kramer, J. R. *Can. J. Anal. Sci. Spectrosc.* **2003**, *48*, 231.
(10) Feller, D.; Glendening, E. D.; de Jong, W. A *J. Chem. Phys.* **1999**, *110*, 1475.
(11) Rosi, M.; Bauschlicher, C. W., Jr. *J. Chem. Phys.* **1990**, *92*, 1876.
(12) Dalleska, N. F.; Honma, K.; Sunderlin, L. S.; Armentrout, P. B. *J. Am. Chem. Soc.* **1994**, *116*, 3519.
(13) Martinez, J. M.; Pappalardo, R. R.; Marcos, E. S. *J. Phys. Chem. A* **1997**, *101*, 4448.
(14) Curtiss, L. A.; Jurgens, R. *J. Phys. Chem. A* **1990**, *94*, 5509.
(15) Armunanto, R.; Schwenk, C. F.; Rode, B. M. *J. Phys. Chem. A* **2003**, *107*, 3132.
(16) Smoes, S.; Mandy, F.; Auwera-Mahieu, A. V.; Drowart, J. *Bull. Soc. Chim. Belges* **1972**, *81*, 45.
(17) Martell, A.; Smith, R. *Critically selected stability constants of metal complexes*; NIST database 46, version 6; NIST, Gaithersburg, MD 20899, 2001.
(18) Phillips, H. O.; Kraus, K. A. *J. Chromatogr.* **1965**, *17*, 549.
(19) Ni, B.; Kramer, J. R.; Werstiuk, N. H. *J. Phys. Chem. A* **2003**, *107*, 2890.
(20) Ni, B.; Kramer, J. R.; Werstiuk, N. H. *J. Phys. Chem. A* **2003**, *107*, 8949.
(21) Frisch, M. J.; Trucks, G. W.; Schlegel, H. B.; Scuseria, G. E.; Robb, M. A.; Cheeseman, J. R.; Zakrzewski, V. G.; Montgomery, J. A.; Stratmann, R. E.; Burant, J. C.; Dapprich, S.; Millam, J. M.; Daniels, A. D.; Kudin, K. N.; Strain, M. C.; Farkas, O.; Tomasi, J.; Barone, V.; Cossi, M.; Cammi, R.; Mennucci, B.; Pomelli, C.; Adamo, C.; Clifford, S.; Ochterski, J.; Petersson, G. A.; Ayala, P. Y.; Cui, Q.; Morokuma, K.; Malick, D. K.; Rabuck, A. D.; Raghavachari, K.; Foresman, J. B.; Cioslowski, J.; Ortiz, J. V.; Stefanov, B. B.; Liu, G.; Liashenko, A.; Piskorz, P.; Komaromi, I.; Gomperts, R.; Martin, R. L.; Fox, D. J.; Keith, T.; Al-Laham, M. A.; Peng, C. Y.; Nanayakkara, A.; Gonzalez, C.; Challacombe, M.; Gill, P. M. W.; Johnson, B. G.; Chen, W.; Wong, M. W.; Andres, J. L.; Head-Gordon, M.; Replogle, E. S. and Pople, J. A. *Gaussian 98*, revision A.9; Gaussian, Inc.: Pittsburgh, PA, 1998.
(22) Perdew, J. P.; Wang, Y. *Phys. Rev. B* **1992**, *45*, 13244.
(23) Godbout, N.; Salahub, D. R.; Andzelm, J.; Wimmer, E. *Can. J. Chem.* **1992**, *70*, 560.
(24) Biegler-Konig, F. *AIM 2000*; University of Applied Science: Bielefeld, Germany, 1998−2000.
(25) Boys, S. F.; Bernardi, F. *Mol. Phys.* **1970**, *19*, 553.
(26) Bader, R. F. W. *Atoms in Molecules*; Oxford Science Publications: Oxford, U.K., 1990.
(27) Gibbs, G. V.; Boisen, M. B.; Beverly, L. L.; Rosso, K. M. *Rev. Mineral. Geochem.* **2002**, *42*, 345.
(28) Schmiedekamp, A. M.; Ryan, M. D.; Deeth, R. J. *Inorg. Chem.* **2002**, *41*, 5733.
(29) Huber, K. P.; Herzberg, G. *Molecular Spectra and Molecular Structure IV. Constants of Diatomic Molecules*; Van Nostrand Reinhold Company: New York, 1979.
(30) Schleyer, P. R. *Encyclopedia of Computational Chemistry*; John Wiley & Sons Ltd.: New York, 1998.
(31) Holland, P. M.; Castleman, A. W. *J. Chem. Phys.* **1982**, *76*, 4195.
(32) Magnera, T. F.; David, D. E.; Michl, J. *J. Am. Chem. Soc.* **1989**, *111*, 4100.
(33) Magnera, T. F.; David, D. E.; Stulik, D.; Orth, R. G.; Jonkman, H. T.; Michl, J. *J. Am. Chem. Soc.* **1989**, *111*, 5036.
(34) Seward, T. M.; Henderson, C. M.; Charnock, J. M.; Dobson, B. R. *Geochim. Cosmochim. Acta* **1996**, *60*, 2273.
(35) Yamaguchi, T.; Lindqvist, O.; Boyce, J. B.; Claeson, T. *Acta Chim. Scand. A* **1984**, *38*, 423.
(36) Ohtaki, H.; Radnai T. *Chem. Rev.* **1993**, *93*, 1157.
(37) Johnsson, M.; Persson, I. *Inorg. Chim. Acta* **1987**, *127*, 43−47.
(38) Sanchez, M. E.; Terryn, B.; Rivail, J. L. *J. Phys. Chem.* **1985**, *89*, 4695.
(39) Jain, D.; Gale, G.; Sapse, A. M. *J. Comput. Chem.* **1989**, *10*, 1031.
(40) Jensen, F. *Introduction to Computational Chemistry*; John Wiley & Sons Ltd.: New York, 1999.
(41) Bonacorsi, R.; Palla, P.; Tomasi, J. *J. Am. Chem. Soc.* **1984**, *106*, 1945.
(42) Pierotti, R. A. *Chem. Rev.* **1976**, *76*, 715.